RESEARCH ARTICLE

Modeling receptor-mediated drug delivery influenced by non-specific binding in stenosed arterial walls with atherosclerotic plaques

Ramprosad Saha[1*], Somnath Choudhury[2]

ABSTRACT

Background: This study aims to examine how non-specific binding affects drug transfer through receptors in atherosclerotic plaques during stent-based delivery. *Hypothesis:* We hypothesize that including non-specific binding and saturable receptor interactions in a quantitative model will lead to more accurate predictions of drug distribution and retention in heterogeneous arterial tissues. *Materials and Methods*: A modeling framework is developed to consider the interactions between dosage, saturable binding, and diffusion, incorporating experimentally determined binding parameters for drug–tissue interactions. Given the diverse nature of the arterial wall—comprising different tissue layers with varying diffusivities—the model integrates drug diffusion, convection, and reaction dynamics within both the plaque and nearby healthy tissue regions. Each tissue layer features free drug, receptor-bound (specific), and non-specifically bound phases, forming a coupled three-phase, two-layer system. The model also accounts for the kinetics of drug-eluting stent (DES) release over time and captures diffusion through the tortuous, porous arterial environment. *Results*: The simulation results show that key parameters such as dissociation constants and the initial drug load in the stent coating greatly influence drug distribution patterns and retention times across different tissue layers. *Conclusion*: This model highlights the important role of non-specific binding and tissue heterogeneity in drug retention during stent-based delivery, offering insights that can help optimize drug-eluting stent design and treatment strategies.

Keywords: Atherosclerosis, Drug-eluting stent, Numericalsimulation.

Indian Journal of Physiology and Allied Sciences (2025); DOI: 10.55184/ijpas.v77i04.533 **ISSN:** 0367-8350 (Print)

INTRODUCTION

Pharmaceutical compounds are usually designed to target specific molecules or groups of related targets. However, in real-world situations, these drugs often bind to a variety of lipids and proteins non-selectively and need to pass through biological membranes to reach their intended action sites. Developing a more accurate, quantitative understanding of how these off-target interactions and transport processes impact drug-target engagement is of great scientific and therapeutic interest. [1-3]

The effectiveness of drug therapy depends on factors such as the amount of drug released, its release profile, the extent of accumulation within tissues [4-6], and the nature of its binding to tissue components. Many studies have examined modeling drug release from stent platforms and tracking the distribution within the artery wall that follows. [7-9]

While these models provide valuable insights—especially in supporting the rationale for controlled, sustained drug release from drug-eluting stents (DES)—they often fall short in replicating clinical outcomes. [10-13] Although theoretical models imply a smooth, continuous relationship between tissue drug concentration, dose, and delivery time, in vivo experiments show that therapeutic efficacy is only reached once specific threshold levels of dose and exposure duration are surpassed. [14-16]

This study investigates how tissue drug content and receptor-mediated responses are affected by the interaction among elution dynamics, tissue transport, and binding to both specific receptors and non-specific proteins. The presence of atherosclerotic plaque near the endothelial surface is also assessed, as it can significantly influence local drug distribution and pharmacokinetics.

Building on a previously proposed single-layer model, this work introduces a more complex, multi-layered framework to better simulate drug transport behavior in diseased arterial tissue. A wide variety of modeling approaches have been developed in the literature, ranging from one-dimensional to more intricate two- and three-dimensional models, built using either simplified or anatomically realistic geometries. These models often involve simplifying assumptions to make analytical or computational solutions possible. Despite these limitations, each model has contributed to advancing

[1]Department of Mathematics, Suri Vidyasagar College, Suri - 731101, Birbhum, West Bengal, India.

[2]Department of Physics, Suri Vidyasagar College, Suri - 731101, Birbhum, West Bengal, India.

***Corresponding author:** Ramprosad Saha, Department of Mathematics, Suri Vidyasagar College, Suri - 731101, Birbhum, West Bengal, India, Email: itsramprasadhere@gmail.com

How to cite this article: Saha R, Choudhury S. Modeling receptor-mediated drug delivery influenced by non-specific binding in stenosed arterial walls with atherosclerotic plaques. *Indian J Physiol Allied Sci* 2025;77(4):48-54.

Conflict of interest: None

Submitted: 05/11/2025 **Accepted:** 19/11/2025 **Published:** 26/12/2025

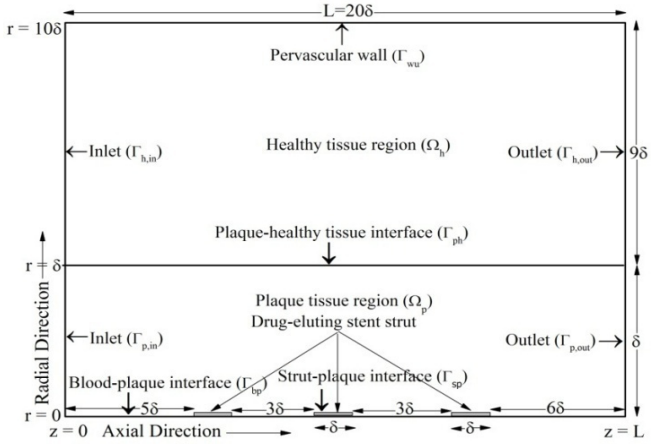

Figure 1: Layout of the computational domain considered

the field—whether by confirming expected outcomes, replicating experimental data, or providing unexpected insights that sparked further refinement of theoretical or experimental methods. However, it remains crucial to ensure that computational simulations are conducted with proper rigor to avoid large uncertainties, which could otherwise undermine the reliability of the results.

MATERIALS AND METHODS

Geometric model

The computational setup is based on a simplified representation of an arterial segment, modeled as a rectangular domain with axial length L, scaled according to the dimensions of the stent strut. It assumes that the artery wall is ten times thicker than the height of the strut, with the plaque occupying a thickness equal to the strut height, and the remaining nine times attributed to healthy tissue layers (Figure 1). [17] A three-phase drug transport framework is used within both the plaque and healthy tissue zones, incorporating free drug, drug bound to specific receptors (SR), and drug bound to extracellular matrix (ECM) components. Free drug movement in both regions is governed by a time-dependent convection-diffusion-reaction mechanism (eqns. 1, 4), while drug interactions with ECM and specific receptors are described by nonlinear, saturable, reversible binding kinetics (eqns. 2, 5 for ECM and eqns. 3, 6 for receptor binding).

Mathematical model and boundary specifications

Zone of arterial plaque buildup

Therefore, the transport equations governing the behavior of free drug, ECM-bound drug, and drug bound to specific receptors (SR-bound) within the plaque-affected area are expressed below using a two-dimensional cylindrical coordinate system asfollows:

$$\frac{\partial Cp_f}{\partial t}+\frac{\gamma_p}{\phi_p}\frac{\partial\left(V_t Cp_f\right)}{\partial r}=Dp_t\left[\frac{\partial^2 Cp_f}{\partial r^2}+\frac{1}{r}\frac{\partial Cp_f}{\partial r}+\frac{\partial^2 Cp_f}{\partial z^2}\right]-\frac{\partial Cp_{be}}{\partial t}-\frac{\partial Cp_{bs}}{\partial t}, \quad (1)$$

$$\frac{\partial Cp_{be}}{\partial t}=kpe_f Cp_f\left(Cpe_{bmax}-Cp_{be}\right)-kpe_r Cp_{be}\ , \quad (2)$$

$$\frac{\partial Cp_{bs}}{\partial t}=kps_f Cp_f\left(Cps_{bmax}-Cp_{bs}\right)-kps_r Cp_{bs}\ . \quad (3)$$

Zone of healthy tissue

In the same manner, the equations governing drug transport in the healthy tissue region can be expressed as:

$$\frac{\partial Ch_f}{\partial t}+\frac{\gamma_h}{\phi_h}\frac{\partial\left(V_t Ch_f\right)}{\partial r}=Dh_t\left[\frac{\partial^2 Ch_f}{\partial r^2}+\frac{1}{r}\frac{\partial Ch_f}{\partial r}+\frac{\partial^2 Ch_f}{\partial z^2}\right]-\frac{\partial Ch_{be}}{\partial t}-\frac{\partial Ch_{bs}}{\partial t}$$

$$\frac{\partial Ch_{be}}{\partial t}=khe_f Ch_f\left(Che_{bmax}-Ch_{be}\right)-khe_r Ch_{be}\ , \quad (5)$$

$$\frac{\partial Ch_{bs}}{\partial t}=khs_f Ch_f\left(Chs_{bmax}-Ch_{bs}\right)-khs_r Ch_{bs}, \quad (6)$$

where Cp_f and Ch_f denote the respective concentrations (in moles per unit tissue volume) of free drug within the plaque and healthy tissue areas; Cp_{be} and Ch_{be} correspond to the ECM-bound drug concentrations (in molar terms) in the plaque and healthy tissue areas, respectively; Cp_{bs} and Ch_{bs} indicate the SR-bound drug concentrations (in molar units) in plaque and healthy tissues, respectively; Cpe_{bmax} and Che_{bmax} correspond to the ECM-binding site densities in the plaque and healthy tissue areas; Cps_{bmax} and Chs_{bmax} correspond to the receptor-binding site densities in the plaque and healthy tissue areas; kpe_f and khe_f represent the forward ECM-binding rate constants in the plaque and healthy tissue regions, respectively; kps_f and khs_f denote the respective forward receptor-binding rate constants in plaque and healthy tissue areas; kpe_r and khe_r denote the respective backward ECM-binding rate constants in plaque and healthy tissue zones; kps_r and khs_r are the backward receptor-binding rate constants in the plaque and healthy tissue areas, respectively and V_t represents the velocity of transmural filtration.

Here, Dq_t denotes the intrinsic diffusivity of the drug within the q^{th} subdomain ($q = p, h$) which can be expressed [18, 20] as:

$$Dq_t=\left[1+\frac{Bq_m}{Kq_d}\right]\times Dq_e \ \ where\ \ Dq_{eff}=\frac{\varepsilon_q}{\tau_q}\times Dq_f$$

In this context, ε_q and τ_q represent the porosity and tortuosity of the wall material [6, 21, 22] respectively, Dq_f and Dq_e denote the free and effective diffusion coefficients, while Bq_m and Kq_d correspond to the net tissue binding capacity and the equilibrium dissociation constant. [22] Throughout this work, ($q=p$) refers to the plaque region, and ($q=h$) denotes the healthy tissue region.

Initial and boundary conditions

As the boundary condition at the blood-plaque interface is not easily determined, the following interface condition was adopted at the blood-plaque interface ($\tilde{A}_{bp}$) as:

$$k_{lw}Jp_f+\left(1-k_{lw}\right)V_t Cp_f=0 \quad on \quad \Gamma_{bp}, \quad (7)$$

where Jp_f refers to the flux at the interface for the free drug, with k_{lw} being a modifiable parameter that offers the flexibility to define a non-trivial boundary condition $(0 \le k_{lw} \le 1)$. When $k_{lw} = 0$, One extreme is when blood is highly effective at removing drug adhered to the vessel wall, represented by a zero-concentration boundary condition. In contrast, when $k_{lw} = 1$, it represents the opposite extreme, where the drug attached to the vessel wall is unaffected by the flow of blood, modeled as a zero-flux boundary condition. For values of k_{lw} between 0 and 1, the condition represents a blend of zero-flux and zero-concentration settings, referred to as a hybrid boundary condition.

Given that stent struts are relatively thin compared to the arterial wall, their detailed geometry is disregarded. Instead, the drug-eluting stent is represented by an idealized or equivalent surface that delivers a specified drug dose to both the arterial lumen and wall (Figure 1).

A time-varying release profile is applied at the interface between the strut and the plaque ($\tilde{A}_{sp}$):

$$Cp_f = C_0 e^{-\lambda t} \quad for \quad t \ge 0 \quad on \quad \Omega_p \cap \Gamma_{bp}, \tag{8}$$

where, λ refers to the drug emission rate from the surfaces of the struts [11] and C_0 is the initial drug concentration in coating. [19]

Symmetry boundary conditions for the free drug are imposed on the proximal ($\tilde{A}_{q,in}$) and distal ($\tilde{A}_{q,out}$) walls within the tissueas:

$$\frac{\partial Cp_f}{\partial z} = 0 \ on \ \ \Gamma_{p,in} \ and \ \Gamma_{p,out}, \tag{9}$$

$$\frac{\partial Ch_f}{\partial z} = 0 \ on \ \ \Gamma_{h,in} \ and \ \Gamma_{h,out}, \tag{10}$$

Appropriate boundary conditions for both forms of the drug are adopted at the plaque–healthy tissue interface ($\tilde{A}_{ph}$) as follows:

$$Dp_t \frac{\partial Cp_f}{\partial r} = Dh_t \frac{\partial Ch_f}{\partial r}, \ \frac{\partial Cp_{be}}{\partial r} = \frac{\partial Ch_{be}}{\partial r} \ and \ \frac{\partial Cp_{bs}}{\partial r} = \frac{\partial Ch_{bs}}{\partial r} \ on \ \Gamma_{ph}. \tag{11}$$

A hybrid boundary condition for the free drug is imposed at the perivascular wall ($\tilde{A}_{wu}$) as:

$$k_{uw} Jh_f + (1 - k_{uw}) V_t Ch_f = 0 \ on \Gamma_{wu}, \tag{12}$$

where k_{uw} functions as a controllable parameter.

Scaling to dimensionless form

Now here it is non-dimensionalized in the manner described below

$$\overline{r} = \frac{r}{r_0}, \ \overline{z} = \frac{z}{\delta}, \ \overline{Cp}_f = \frac{Cp_f}{C_0}, \ \overline{Ch}_f = \frac{Ch_f}{C_0}, \ \overline{Cp}_{be} = \frac{Cp_{be}}{Cpe_{bmax}},$$

$$\overline{Cp}_{bs} = \frac{Cp_{bs}}{Cps_{bmax}}, \ \overline{Ch}_{be} = \frac{Ch_{be}}{Che_{bmax}}, \ \overline{Ch}_{bs} = \frac{Ch_{bs}}{Chs_{bmax}}, \ \overline{t} = \frac{tV_t}{\delta},$$

Based on these assumptions, the equations 1–12 can be reformulated in their nondimensional forms, with the bar notation omitted, as shown below:

$$\frac{\partial Cp_f}{\partial t} = \frac{\epsilon \gamma_p}{\epsilon_p} \frac{\partial Cp_f}{\partial r} + \frac{\epsilon}{Pe_p} \left[\frac{\partial^2 Cp_f}{\partial r^2} + \frac{1}{r} \frac{\partial Cp_f}{\partial r} + \frac{1}{\epsilon^2} \frac{\partial^2 Cp_f}{\partial z^2} \right] - \frac{1}{\beta p_e} \frac{\partial Cp_{be}}{\partial t} - \frac{1}{\beta p_s} \frac{\partial Cp_{bs}}{\partial t} \tag{13}$$

$$\frac{\partial Cp_{be}}{\partial t} = \frac{Da_{pe} \beta p_e}{\epsilon Pe_p} \left(Cp_f (1 - Cp_{be}) - \alpha_{pe} Cp_{be} \right) \tag{14}$$

$$\frac{\partial Cp_{bs}}{\partial t} = \frac{Da_{ps} \beta p_s}{\epsilon Pe_p} \left(Cp_f (1 - Cp_{bs}) - \alpha_{ps} Cp_{bs} \right) \tag{15}$$

$$\frac{\partial Ch_f}{\partial t} = \frac{\epsilon \gamma_h}{\epsilon_h} \frac{\partial Ch_f}{\partial r} + \frac{\epsilon}{Pe_h} \left[\frac{\partial^2 Ch_f}{\partial r^2} + \frac{1}{r} \frac{\partial Ch_f}{\partial r} + \frac{1}{\epsilon^2} \frac{\partial^2 Ch_f}{\partial z^2} \right] - \frac{1}{\beta h_e} \frac{\partial Ch_{be}}{\partial t} - \frac{1}{\beta h_s} \frac{\partial Ch_{bs}}{\partial t} \tag{16}$$

$$\frac{\partial Ch_{be}}{\partial t} = \frac{Da_{he} \beta h_e}{\epsilon Pe_h} \left(Ch_f (1 - Ch_{be}) - \alpha_{he} Ch_{be} \right) \tag{17}$$

$$\frac{\partial Ch_{bs}}{\partial t} = \frac{Da_{hs} s}{\epsilon Pe_h} \left(Ch_f (1 - Ch_{bs}) - \alpha_{hs} Ch_{bs} \right) \tag{18}$$

$$k_{lw} Jp_f + \frac{(1 - k_{lw})}{Pe_p} Cp_f = 0 \quad on \quad \Gamma_{bp} \tag{19}$$

$$Cp_f = e^{-\lambda_N t} \quad for \quad t \ge 0 \quad on \quad \Omega_p \cap \Gamma_{bp}, \tag{20}$$

$$\frac{\partial Cp_f}{\partial z} = 0 \ on \ \ \Gamma_{p,in} \ and \ \Gamma_{p,out}, \tag{21}$$

$$\frac{\partial Ch_f}{\partial z} = 0 \ on \ \ \Gamma_{h,in} \ and \ \Gamma_{h,out}, \tag{22}$$

$$\frac{\partial Cp_f}{\partial r} = Dh / p_t \frac{\partial Ch_f}{\partial r}, \ \frac{\partial Cp_{be}}{\partial r} = \frac{\partial Ch_{be}}{\partial r} \ and \ \frac{\partial Cp_{bs}}{\partial r} = \frac{\partial Ch_{bs}}{\partial r} \ on \ \Gamma_{ph}. \tag{23}$$

$$k_{uw} Jh_f + \frac{(1 - k_{uw})}{Pe_h} Ch_f = 0 \ on \Gamma_{wu}, \tag{24}$$

where the dimensionless parameters are as follows:

$$\epsilon = \frac{\delta}{r_0}, \ \lambda_N = \frac{\lambda \delta}{V_t}, \ Pe_p = \frac{r_0 V_t}{Dp_t}, \ Pe_h = \frac{r_0 V_t}{Dh_t}, \ Da_{pe} = \frac{kpe_f Cpe_{bmax} \delta^2}{Dp_t}, \ Da_{ps} = \frac{kps_f Cps_{bmax} \delta^2}{Dp_t},$$

$$Da_{he} = \frac{khe_f Che_{bmax} \delta^2}{Dh_t}, \ Da_{hs} = \frac{khs_f Chs_{bmax} \delta^2}{Dh_t}, \ \alpha_{pe} = \frac{kpe_r}{C_0 kpe_f}, \ \alpha_{ps} = \frac{kps_r}{C_0 kps_f},$$

$$\alpha_{he} = \frac{khe_r}{C_0 khe_f}, \ \alpha_{hs} = \frac{khs_r}{C_0 khs_f}, \ \beta p_e = \frac{C_0}{Cpe_{bmax}}, \ \beta p_s = \frac{C_0}{Cps_{bmax}},$$

$$\beta h_e = \frac{C_0}{Che_{bmax}}, \ \beta h_s = \frac{C_0}{Chs_{bmax}}.$$

Change of variables in the radial direction

Rescaling of the domain is carried out using the transformations below

$$\xi = 1 + \frac{r - R_{tl}}{R_{tm} - R_{tl}} = 1 + \frac{r - R_{tl}}{R_{tml}} \ and \ \eta = 2 + \frac{r - R_{tm}}{R_{tu} - R_{tm}} = 2 + \frac{r - R_{tm}}{R_{tum}} \tag{25}$$

This transformation resizes the plaque domain to $[0, L] \times [1, 2]$ and the healthy tissue domain to $[0, L] \times [2, 3]$. Here, $R_{tl} = \tilde{A}_{bp} \cup \tilde{A}_{sp}$, $R_{tm} = \tilde{A}_{ph}$, $R_{tu} = \tilde{A}_{wu}$, $R_{tml} = R_{tm} - R_{tl}$ and $R_{tum} = R_{tu} - R_{tm}$. All governing equations, along with the specified boundary conditions (eqns 13-24), are now expressed in dimensionless form.

Table 1: Reasonable dimensional estimates of the relevant parameters

Descriptions	*Involved parameters*			
Strut dimension [3,4]	$\delta = 0.01cm$			
Artery radius [3, 4]	$r_0 = 15 \times \delta$			
Thickness of artery [3, 4]	$W = 10 \times \delta$			
Thickness of plaque [6]	$W_p = 2 \times \delta$			
Thickness of healthy tissue [6]	$W_h = 8 \times \delta$			
Initial drug load in the coating [19]	$C_0 = 10^{-8} mol / cm^3$			
Stent's drug release rate [14]	$ë = 10^{-5} \sec^{-1}$			
Tissue filtration velocity [12, 16]	$V_t = 5.8 \times 10^{-6} cm / sec$			
Descriptions	Plaque zone		Healthy tissue zone	
Hindrance coefficient	$\gamma_p = 1$	[6, 22]	$\gamma_h = 1$	[6]
Porosity	$\dot{o}_p = 0.61$	[6, 22]	$\dot{o}_h = 0.61$	[6]
Tortuosity	$\tau_p = 1.333$	[20, 22]	$\tau_h = 1.333$	[20]
Drug diffusivity, cm^2 / sec	$Dp_t = 1.65 \times 10^{-8}$	[18, 22]	$Dh_t = 8.0 \times 10^{-8}$	[18]
Forward ECM- binding rate, $\left(mol.cm^{-3}.sec\right)^{-1}$	$kpe_f = 2.0 \times 10^6$	[22]	$khe_f = 2.0 \times 10^6$	[13]
Forward SR- binding rate, $\left(mol.cm^{-3}.sec\right)^{-1}$	$kps_f = 8.0 \times 10^8$	[22]	$khs_f = 8.0 \times 10^8$	[13]
Total tissue binding capacity, mol / cm^3	$Bp_m = 3.66 \times 10^{-7}$	[This study]	$Bh_m = 3.66 \times 10^{-7}$	[23]
ECM- binding site density, mol / cm^3	$Cpe_{bmax} = 3.63 \times 10^{-7}$	[This study]	$Che_{bmax} = 3.63 \times 10^{-7}$	[13]
SR- binding site density, mol / cm^3	$Cps_{bmax} = 3.3 \times 10^{-9}$	[This study]	$Chs_{bmax} = 3.3 \times 10^{-9}$	[13]
Equilibrium dissociation constant, mol / cm^3	$Kp_d = 1.3 \times 10^{-9}$	[22]	$Kh_d = 1.3001 \times 10^{-9}$	[23]
Backward ECM- binding rate, sec^{-1}	$kpe_r = 5.2 \times 10^{-3}$	[22]	$khe_r = 5.2 \times 10^{-3}$	[13]
Backward SR- binding rate, sec^{-1}	$kps_r = 1.6 \times 10^{-4}$	[22]	$khs_r = 1.6 \times 10^{-4}$	[13]

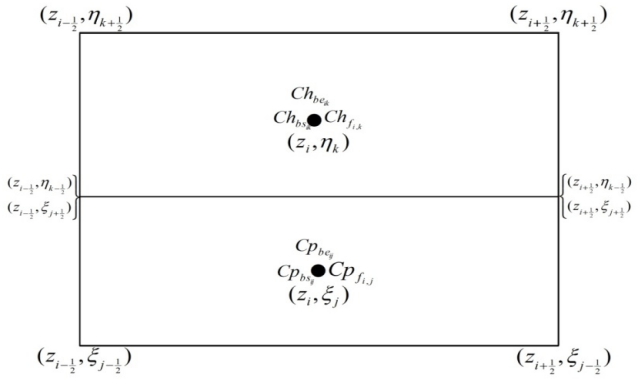

Figure 2: A hybrid MAC cell for both plaque and healthy tissue zones

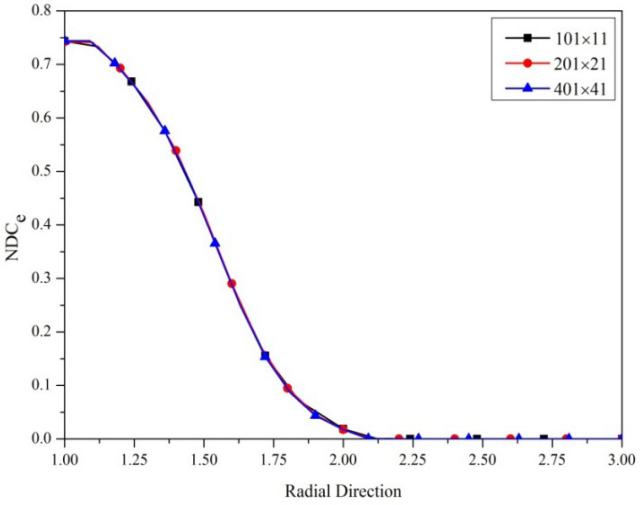

Figure 3: Transmural changes of normalized drug concentration in ECM-bound phase (NDC_e) for various grid sizes at $z=9.5$ and NDT = 10

Solving Methodology

The governing equations, along with the initial and boundary conditions, are solved numerically using a finite-difference scheme. The explicit numerical scheme employs a forward-time centered-space discretization technique. In this scheme, $z_i = i\delta z,\ \xi_j = j\delta\xi,\ \eta_k = k\delta\eta \ and\ t_n = n\delta t$ where *n* represents the time level, δt is the time increment, and δz is the spatial step size along the axial direction (Figure 2). Additionally, $\delta\xi$ and $\delta\eta$ represent the spatial step sizes along the radial direction in the plaque and healthy tissue zones, respectively. The discretized equations are solved numerically using an explicit approach. Instead of relying on a standard software package, the computational code has been custom-programmed in FORTRAN.

RESULTS AND DISCUSSION

A comprehensive quantitative analysis has been carried out using graphical illustrations, based on the parameter values listed in Table 1. To perform the numerical computations of the relevant quantities, the computational domain is limited to a finite non-dimensional length L, with solutions calculated using a grid size of 201×21. A grid-independence study was conducted to assess the error associated with different grid sizes, and the results are presented in Figure 3. The transmural variations of the normalized drug concentration (NDC) in the ECM-bound phase at an axial distance of $z=9.5$ for three different grid sizes ($101\times11, 201\times21$, and 401×41) show near-perfect overlap, confirming the accuracy of the chosen grid sizes.

Figure 4$(a-c)$ illustrate the transmural changes of free drug (NDC_f), drug bound to ECM-binding site (NDC_e), and drug bound to SR-binding sites (NDC_s) at three distinct non-dimensional times. The drug begins to enter the arterial wall at $\xi=1$ in the free phase and quickly binds to both ECM and SR sites. It is important to note that the penetration depth of both the free drug and ECM-bound drug increases over time, with binding site saturation eventually occurring. Additionally, the SR-bound drug is absorbed at the adventitial boundary ($\eta=3$) as time progresses. By $NDT=50$, both the free drug (NDC_f) and ECM-bound drug (NDC_e) have penetrated half the thickness of the tissue. While the profiles of NDC_f and NDC_e are similar, drug concentrations in the SR-bound phase are higher than those in the ECM-bound phase. Over time, the SR-bound drug becomes saturated, as shown in Figure 4(c). These findings are consistent with those of Tzafriri *et al.* [21]

Figure 5 $(a-c)$ illustrates the impact of the scaling parameter α_{pe}, which is directly related to the equilibrium dissociation constant Kp_d at the ECM-binding site, on the temporal changes in normalized mean concentrations (NMC) within the plaque region. The figures show that, unlike NDC_e (Figure 5b), both NDC_s (Figure 5c), and NDC_f (Figure 5a) decrease as α_{pe} decreases. Additionally, Figure 5c highlights that NMC_s increases rapidly over time and reaches a steady state for both higher and lower values of α_{pe}. It is evident that the concentrations of free drug and ECM-bound drug within the plaque region, shown in Figures 5a and 5b, respectively, rise quickly from zero to a maximum value, with the free drug decaying faster than the ECM-bound drug over time. Notably, the peak of NDC_s is reached more quickly than that of NDC_e, and a greater amount of drug is present in the SR-bound phase compared to the other two phases. Similar trends are observed in the healthy tissue region as well (Figure 6a-6c). Figures 5 and 6 clearly show that the normalized mean drug concentrations for free, ECM-bound, and SR-bound drugs in the plaque region are consistently higher and reach their maximum values more quickly than in the healthy tissue region. Additionally, as the equilibrium dissociation constants kp_d and kh_d decrease, receptor occupancy initially drops but increases over time for both SR-bound and free drugs in both regions. In contrast, the ECM-bound drug follows an opposite trend in both regions. Figure 5(c) and Figure 6 (c) demonstrate that receptor binding is hindered at both very high and very low values of the equilibrium dissociation constant. At extremely low values, plasma-protein binding

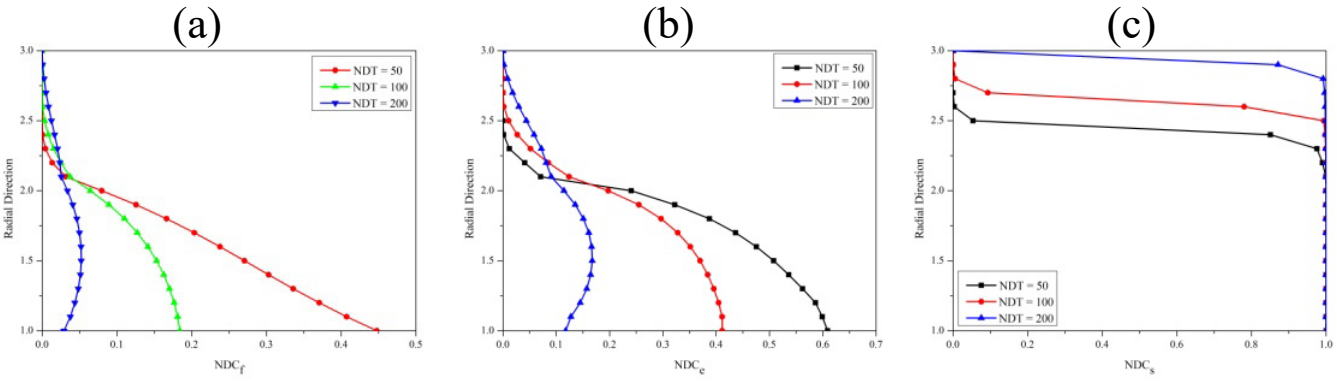

Figure 4: Transmural changes of normalized drug concentration for variousnon-dimensional times at $z = 9.5$. (a) Normalized free drug concentration (NDC_f), (b) Normalized drug concentration in ECM-bound phase (NDC_e), and (c) Normalized drug concentration in SR-bound phase (NDC_s).

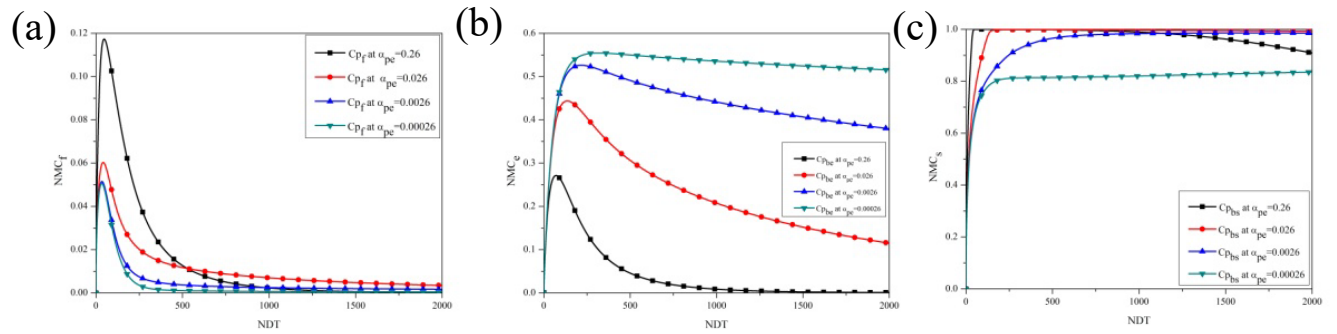

Figure 5: Temporal variation of the normalized mean concentration in the plaque region for different α_{pe}. (a) Normalized mean free drug concentration (NMC_f), (b) Normalized mean drug concentration in ECM-bound phase (NMC_e), and (c) Normalized mean drug concentration in SR-bound phase (NMC_s)

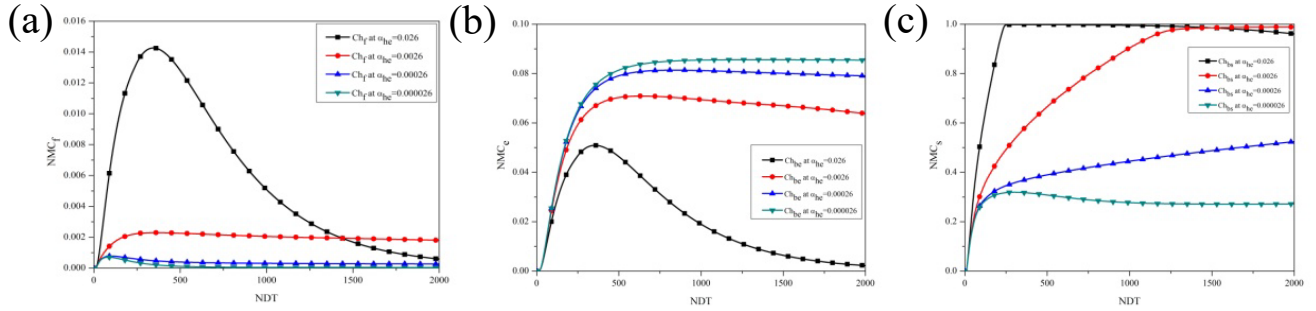

Figure 6: Temporal variation of normalized mean concentration in the healthy tissue different α_{he} (a) Normalized mean free drug concentration (NMC_f), (b) Normalized mean drug concentration in ECM-bound phase (NMC_e), and (c) Normalized mean drug concentration in SR-bound phase (NMC_s)

prevails, leaving no free drug available for receptor binding. At very high values, drug clearance dominates, and the drug is eliminated from the plasma before it can bind to receptors. Consequently, an optimal intermediate value of the equilibrium dissociation constant exists for both the plaque and healthy tissue regions, a finding that aligns with the work of Peletier *et al.* [20]

CONCLUSION AND FUTURE RESEARCH DIRECTION

A deeper understanding of drug release kinetics and tissue absorption is crucial for effectively optimizing stent-based drug delivery systems. One way to evaluate the characteristics of drug elution from a drug-eluting stent (DES) into the arterial wall and to fine-tune the physicochemical parameters is

through mathematical modeling and numerical simulations. In this paper, an existing model is extended, focusing on reversible and saturable binding processes in both vascular plaque and healthy tissue. The model depicts a two-layer, multi-phase system, where partial differential equations govern the unsteady convection-reaction-diffusion process for the free drug, while bound drugs are modeled as reaction-only processes in both plaque and healthy tissue regions. Simulation results indicate that binding sites become saturated over time, with the SR-bound drug being fully absorbed at the adventitial boundary.

CONFLICT OF INTEREST

The authors declare no conflicts of interest in connection with this publication.

REFERENCES

1. Balakrishnan B, Dooley J, Kopia G, Edelman ER. Thrombus causes fluctuations in arterial drug delivery from intravascular stents. *J Control Release*. 2008;131(3):173–80. DOI: 10.1016/j.jconrel.2008.07.027.
2. Balakrishnan B, Tzafriri AR, Seifert P, Groothuis A, Rogers C, Edelman ER. Strut position, blood flow, and drug deposition implications for single and overlapping Drug-Eluting Stents. *Circulation*. 2005;111(22):2958–65. DOI: 10.1161/CIRCULATIONAHA.104.512475.
3. Berezhkovskiy LM. On the influence of protein binding on pharmacological activity of drugs. *J Pharm Sci*. 2010;99(4):2153–65. DOI: 10.1002/jps.21958.
4. Schmidt S, Gonzalez D, Derendorf H. Significance of protein binding in pharmacokinetics and pharmacodynamics. *J Pharm Sci*. 2010;99(3):1107–22. DOI: 10.1002/jps.21916.
5. Serruys PW, Sianos G, Abizaid A, *et al*. The effect of variable dose and release kinetics on neointimal hyperplasia using a novel paclitaxel-eluting stent platform: the Paclitaxel In-Stent Controlled Elution Study (PISCES). *J Am Coll Cardiol*. 2005;46(2):253–60. DOI: 10.1016/j.jacc.2005.03.069.
6. Tzafriri AR, Groothuis A, Price GS, Edelman ER. Stent elution rate determines drug deposition and receptor-mediated effects. *J Control Release*. 2012;161(3):918–26. DOI: 10.1016/j.jconrel.2012.05.039.
7. McGinty S, McKee S, McCormick C, Wheel M. Release mechanism and parameter estimation in drug-eluting stent systems: analytical solutions of drug release and tissue transport. *Math Med Biol*. 2014;32(2):163–86. DOI:10.1093/imammb/dqt025.
8. McGinty S, McKee S, Wadsworth RM, McCormick C. Modelling drug-eluting stents. *Math Med Biol*. 2011;28(1):1–29. DOI: 10.1093/imammb/dqq003.
9. McGinty S, Pontrelli G. A general model of coupled drug release and tissue absorption for drug delivery devices. *J Control Release*. 2015;217:327–36. DOI: 10.1016/j.jconrel.2015.09.025.
10. Gershlick A, De Scheerder I, Chevalier B, *et al*. Inhibition of restenosis with a paclitaxel-eluting, polymer-free coronary stent: the European evaLUation of pacliTaxel Eluting Stent (ELUTES) trial. *Circulation*. 2004;109:487–93. DOI: 10.1161/01.CIR.0000109694.58299.A0.
11. Hausleiter J, Kastrati A, Wessely, *et al*. Randomized, double-blind, placebo-controlled trial of oral sirolimus for restenosis prevention in patients with in-stent restenosis: the Oral Sirolimus to Inhibit Recurrent In-stent Stenosis (OSIRIS) trial. *Eur Heart J*. 2005;26:1475–81. DOI: 10.1161/01.CIR.0000138935.17503.35.
12. Hausleiter J, Kastrati A, Wessely R, *et al*. Prevention of restenosis by a novel drug-eluting stent system with a dose-adjustable, polymer-free, on-site stent coating. *Eur Heart J*. 2005;26:1475–81. DOI: 10.1093/eurheartj/ehi405.
13. Huang ZJ, Tarbell JM. Numerical simulation of mass transfer in porous media of blood vessel walls. *Am J Physiol*. 1997;273(1 Pt 2):H464-77. DOI: 10.1152/ajpheart.1997.273.1.H464.
14. McGinty S, Pontrelli G. On the role of specific drug binding in modelling arterial eluting stents. *J Math Chem*. 2016;54(4):967–76. DOI: 10.1007/s10910-016-0618-7.
15. Mongrain R, Faik I, Leask RL, Rod'C J, Bertrand OF, others. Effects of diffusion coefficients and struts apposition using numerical simulations for drug eluting coronary stents. *J Biomech Eng*. 2007;129(5):733–42. DOI: 10.1115/1.2768381.
16. O'Brien C, Kolachalama V, Barber T, Simmons A, Edelman E. Impact of flow pulsatility on arterial drug distribution in stent-based therapy. *J Control Release*. 2013;168(2):115–24. DOI: 10.1016/j.jconrel.2013.03.014.
17. Ferdous J, Chong CK. Effect of Atherosclerotic Plaque on Drug Delivery from Drug-eluting Stent. *In: 13th International Conference on Biomedical Engineering*. 2009. p. 1519–22. DOI:10.1007/978-3-540-92841-6_376. DOI: 10.1007/978-3-540-92841-6_376.
18. Kolachalama VB, Pacetti SD, Franses JW, *et al*. Mechanisms of tissue uptake and retention in zotarolimus-coated balloon therapy. *Circulation*. 2013;127(20):2047–55. DOI: 10.1161/CIRCULATIONAHA.113.002051.
19. O'Connell BM, Walsh MT. Demonstrating the influence of compression on artery wall mass transport. *Ann Biomed Eng*. 2010;38(4):1354–66. DOI: 10.1007/s10439-010-9914-8.
20. Peletier LA, Benson N, Graaf PH van der. Impact of plasma-protein binding on receptor occupancy: An analytical description. *J Theor Biol*. 2009;256:253–62. DOI: 10.1016/j.jtbi.2008.09.014.
21. Tzafriri AR, Levin AD, Edelman ER. Diffusion-limited binding explains binary dose response for local arterial and tumour drug delivery. *Cell Prolif*. 2009;42(3):348–63. DOI: 10.1111/j.1365-2184.2009.00602.x.
22. Vairo G, Cioffi M, Cottone R, Dubini G, Migliavacca F. Drug release from coronary eluting stents: a multidomain approach. *J Biomech*. 2010;43(8):1580–9. DOI: 10.1016/j.jbiomech.2010.01.033.
23. Tedgui A, Lever MJ. Filtration through damaged and undamaged rabbit thoracic aorta. *AmJ Physiol Circ Physiol*. 1984;247(5):H784--H791. DOI: 10.1152/ajpheart.1984.247.5.h784.

PEER-REVIEWED CERTIFICATION

During the review of this manuscript, a double-blind peer-review policy has been followed. The author(s) of this manuscript received review comments from a minimum of two peer-reviewers. Author(s) submitted revised manuscript as per the comments of the assigned reviewers. On the basis of revision(s) done by the author(s) and compliance to the Reviewers' comments on the manuscript, Editor(s) has approved the revised manuscript for final publication.